

High Quality Autostereoscopic Surgical Display Using Anti-aliased Integral Videography Imaging

Hongen Liao, Daisuke Tamura, Makoto Iwahara, Nobuhiko Hata, and
Takeyoshi Dohi

Graduate School of Information Science and Technology, the University of Tokyo
7-3-1 Hongo, Bunkyo-ku, Tokyo 113-8656, Japan
liao@atres.t.u-tokyo.ac.jp

Abstract. This paper presents an autostereoscopic three-dimensional (3-D) surgical display with high quality integral videography (IV) rendering algorithm. IV is an animated extension of integral photography, which provides 3-D images without using any supplementary glasses or tracking devices. Despite IV's many advantages, the quality of its spatial image has thus far been poor. We developed a high quality image rendering method with oversampling technique for enhancing the resolution of elemental IV image and low-pass-filter for smoothing the image. Furthermore, we manufactured a high-resolution IV display for evaluating the feasibility of proposed method. The experimental results show the quality of anti-aliased IV image is improved. We also integrated the developed IV image into image-guided surgery display system. This approach will allow us to acquire the optimum process to produce high quality 3-D image for planning and guidance of minimally invasive surgery.

1 Introduction

The objective of the image-guided surgery is to enhance the surgeon's capability to utilize medical imagery to decrease the invasiveness of surgical procedures and increase their accuracy and safety. The display used for the surgical navigation system is often placed in a nonsterile field from surgeon. These force the surgeon to take extra steps to match guidance information on the display with the actual anatomy of the patient. This hand-eye coordination problem has been discussed as possible cause of the interruption of surgical flow [1]. Furthermore, most of medical information in pre- or intra-operative image to surgeons, as a set of 2-D sectional images displayed away from the surgical area. This reconstructed 3-D information sometimes differs between individual surgeons.

Stereoscopic technique has been taking an important roll in surgery and diagnosis with various modes of visualization on offer [2-3]. Among previous reported stereoscopic techniques use polarized or shuttering glasses to create 3-D image for surgical simulation and diagnosis. This binocular stereoscopic display reproduces the depth of projected objects by using fixed binoculars; because the images for the left and right eyes are formed separately, there is a disparity in the reproduced image. Therefore, different viewers can have inconsistent depth perception [4]. Not much has

been done to investigate the negative impact of this inconsistency on the accuracy of surgical navigation.

We have developed an autostereoscopic imaging technique, in contrast to a binocular stereoscopic display, that can be integrated into a surgical navigation system by superimposing an actual 3-D image onto the patient. The autostereoscopic images are created by using a modified version of integral videography (IV), which is an animated extension of the integral photography (IP) proposed by Lippmann [5]. IP and IV record and reproduce 3-D images using a micro convex lens array and photographic film (or a flat display). A high-resolution multi-projection IV display system [6] and a surgical navigation system by IV image overlay [7] are introduced for image-guided surgery. With additional improvements in the display, these systems will increase the surgical accuracy and reduce invasiveness.

Despite IV's many advantages that have been proven in both feasibility studies and clinical applications [6-8], the quality of its spatial image has thus far been poor. Furthermore, a high quality 3-D visualization system must be developed to integrate capabilities for pre-surgical/intra-operative image guidance. In this study, we describe an anti-aliased image rendering algorithm for high quality IV image generation. The high-quality rendering method is developed for each elemental image of IV by using oversampling technique to enhance the resolution of element images and low-pass-filter to smooth the resultant images. We further manufactured a high-resolution IV display for evaluating the feasibility of the proposed method.

2 Materials and Methods

2.1 Original IV Image Rendering Method

IV uses a fast image rendering algorithm to project a computer-generated graphical object through a micro-convex lens array. Each point shown in a 3-D space is reconstructed at the same position as the actual object by the convergence of rays from the pixels of the elemental images on the computer display after they pass through the lenslets in the lens array. The surgeon can see the object on the display from various directions, as though it were fixed in 3-D space.

Because resolution of flat display is much lower than that of photographic film (used in the original method of IP), there is a decrease in the amount of information displayed. Thus, all points on a 3-D object cannot be displayed on flat display, and only the 3-D information of the points most suitable to each pixel of the computer display must be processed.

The coordinates of the points in the 3-D object that correspond to each pixel on the screen must be computed for each pixel on the display (Fig. 1). The procedure is similar to the ray-tracing algorithm, although the tracings in this instance are directly opposite those observed on the screen. Our algorithm creates 3-D objects in the space between the screen and the observer, while the ray-tracing algorithm would place the object behind the screen. Unlike natural objects, information about any point in the original object can be directly acquired in the case of medical 3-D images, making our method free from the pseudoscopic image problems peculiar to IP.

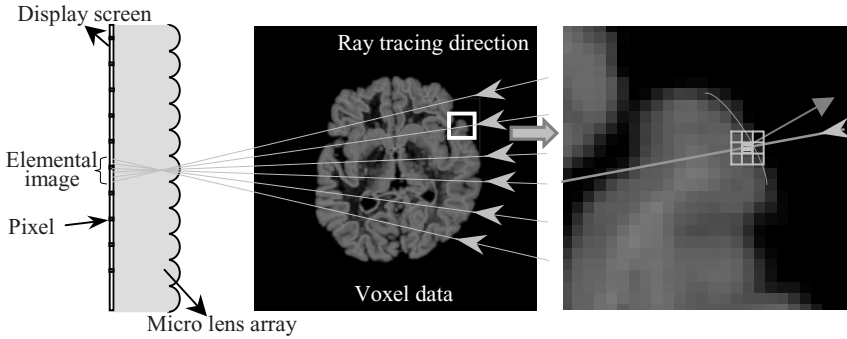


Fig. 1. Fundamental IV rendering algorithm.

2.2 Quality Improvement of IV Elemental Image by Anti-aliased Algorithm

The limited resolution of flat display cause several problems. Because the depth information is encoded into the 2-D image, the projected image of this into 3-D space has a much lower resolution. The aliasing appear when we use a low-density ray tracing (low sampling frequency) algorithm and display resultant IV elemental image in a low-resolution display. There were a large number of different techniques in anti-aliasing in the computer graphics community and medical field [9-11].

The relationship between the pixels in the elemental image is considered for generating the pixel. The entire image information surrounding to the voxel data tracked by ray tracing is used for pixel calculation when the single pixel of the elemental image is rendered (Fig. 2). We introduce a modified oversampling image processing method for anti-aliased IV rendering.

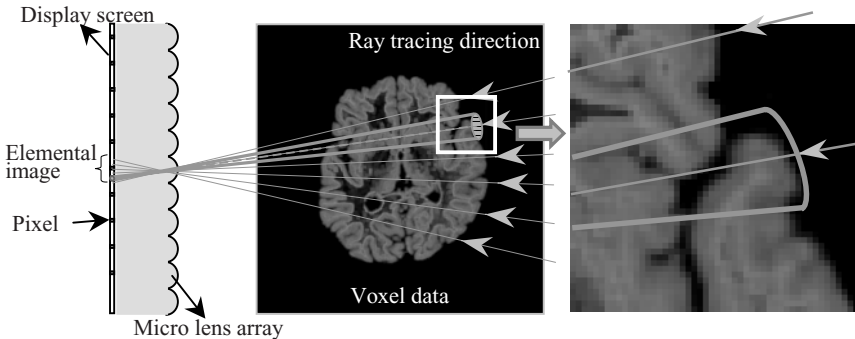


Fig. 2. Oversampling ray tracing method for rendering IV elemental image.

Assuming the lens pitch and the pixel pitch of display to be p and P_p , respectively, and each lens covers N_p pixels, the width of each elemental image is $W_p = N_p \times P_p$. The voxel data is putted in the space with a mm and b mm in front of and behind the lens array, respectively (Fig. 3). The maximum rendering area of the voxel data in position

a for each elemental image is W_v mm, which covers N_v voxel number with each voxel pitch of V_p , then $W_v = N_v \times V_p$.

The focal length of lenslet is h , the relationship between the W_p and W_v is $W_v = W_p \times a/h$. The covered voxel numbers in position a is given by

$$N_v = \frac{W_v}{V_p} = \frac{a \times W_p}{h \times V_p} \quad (1)$$

A signal sampled at a frequency higher than the pixel number of elemental image (Nyquist frequency in the ray tracing) is said to be oversampled β times, where the oversampling ratio of the voxel number to pixel number is defined as

$$\beta = \frac{N_v}{N_p} = \frac{a \times P_p}{h \times V_p} \quad (2)$$

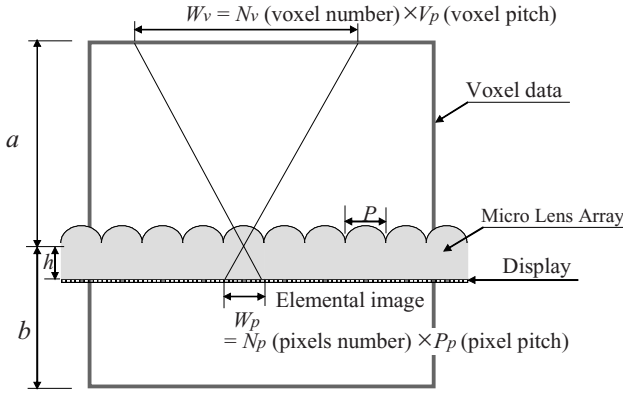


Fig. 3. Relationship between the pixel of elemental image and voxel data.

Considering the maximum position of voxel data corresponding to the lens array and the spatial relationship between the voxel data and the lens array, the oversampling ratio is modified as

$$\beta = \frac{\max(a, b) \times P_p}{h \times V_p \times \cos \theta} \quad (3)$$

where θ is an intersected angle between the voxel and lens array.

Although the resolution of elemental image is increased, the display only provides limited pixels for each elemental image. It is necessary to keep the high quality of image and drop the image resolution as it can be displayed in IV display. A low-pass-filter imaging method with Fourier transform is proposed to solve this problem.

Assuming the resolution of display is $m \times n$ pixels and the oversampling ratio is β , the number of ray tracing for IV image rendering will be $(m \times \beta) \times (n \times \beta)$. A Discrete Fourier Transformation is used for image transform. The spectrum function of $F(u, v)$ is expressed as

$$F(u, v) = \sum_{x=0}^{m \times \beta - 1} \sum_{y=0}^{n \times \beta - 1} f(x, y) \exp\left(-j \frac{2\pi x}{m \times \beta} u - j \frac{2\pi y}{n \times \beta} v\right), \quad (4)$$

where $f(x,y)$ is brightness value function of the pixel in position (x,y) , u and v are the frequencies of image in x and y direction, respectively. The output of oversampled elemental image is low-pass filtered and decimated to achieve a necessary frequency component of image with the target pixel count by using

$$F'(u,v) = F(u,v) * \delta_{u,v}, \tag{5}$$

where $\delta_{u,v}$ is a delta function. We extract the central oversampled image to $(m \times n)$ pixels.

$$F(s,t) = F\left(\frac{m * \beta}{2} - m + 1 + s, \frac{n * \beta}{2} - n + 1 + t\right); \quad (s \in [0, m-1], t \in [0, n-1]). \tag{6}$$

Last, transform the resultant spectrum to normal image corresponding to each elemental image by using a Reverse Discrete Fourier Transformation.

$$f(x,y) = \frac{1}{m} \frac{1}{n} \sum_{s=0}^{m-1} \sum_{t=0}^{n-1} F(s,t) \exp\left(j \frac{2\pi s}{m} x + j \frac{2\pi t}{n} y\right). \tag{7}$$

We compare the high quality elemental image using above algorithm (Fig. 4b) with that of the fundamental rendering method (Fig. 4a). The novel rendering method creates an anti-aliased element IV image with higher quality for spatial IV image formation.

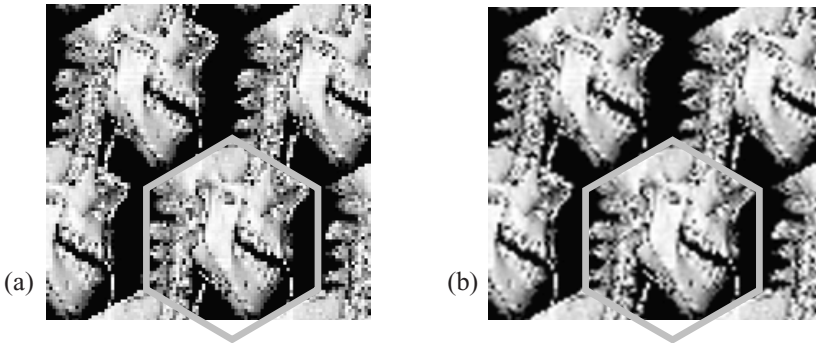


Fig. 4. High quality image rendering method for elemental IV image (hexagon lens); a) Fundamental IV rendering method. b) Modified oversampling algorithm for anti-aliased image.

2.3 High-Resolution IV Autostereoscopic Display

The IV display we developed consists of a high-resolution LCD with a micro convex lens array. The quality of the IV image depends primarily on the pixel density of the display (the number of pixels per unit display area) and the lens pitch of the lens array. The LCD display (IBM, T221) is with 3840×2400 pixels on a size of 460.8×288.0 mm (200ppi). The pitch of each pixel on the screen is 0.085 mm. Each lenslet element is hexagonal with a base area of 1.486 mm in width and 1.238 mm in height, which covers 12×10 pixels of the projected image. The focal length of the lenslet is 2.4 mm. Photographs of IV display device and motion parallax of displayed IV image.

3 Experiments and Results

3.1 IV Image Quality Evaluation

We evaluated the feasibility of proposed method by using a zoneplate (Fig. 5a) displayed in front of the lens array. The image brightness of zoneplate is defined as:

$$A \times \sin \left\{ \frac{\pi}{2} \left(\frac{(x-a)^2}{\alpha} + \frac{(y-b)^2}{\beta} \right) + \Theta \right\} + B \tag{8}$$

where (x, y) is the position of image, (a, b) is center of concentric circle. (α, β) is the radius of the concentric circle in maximum resolution. A is an amplitude of a sine wave. B is an overlaid gray level of the sine wave. Θ is a phase of sine wave in the concentric circle.

Figure 5c show an IV images of zoneplate by using anti-aliased technique. The aliasing images disappear in area A and B compared with the image using original rendering method as shown in Fig. 5b.

Figure 6 give the measured results between the frequency of observed alias and the oversampling ratio. By analyzing the frequency of IV image processing, we found the IV rendering algorithm can be improved for a high-quality IV image generating.

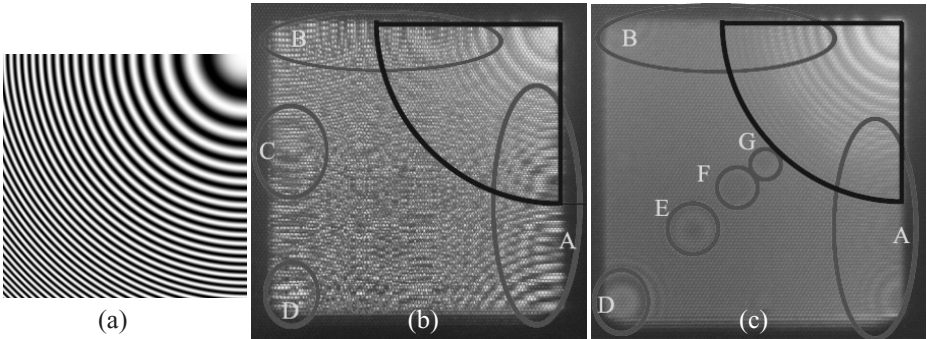


Fig. 5. IV autostereoscopic image: (a) zone plate used for evaluating the image quality. (b) Original IV rendering result, $\beta=1$; the aliasing images appear in area A, B, C, and D. (c) IV image using oversampling and low-pass-filter, $\beta=20$.

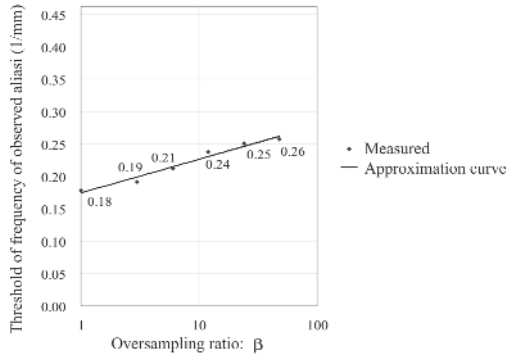


Fig. 6. Relationship between the frequency of observed alias and the oversampling ratio.

3.2 Feasibility Evaluation for Image-Guided Surgery

We evaluated the usefulness of the developed method. In clinical feasibility study, we performed CT scanning to take photo of in-vivo skull. The volumetric CT images of skull (256×256 pixels \times 94 slices, thickness of 2.0mm) were rendered and displayed in high-resolution IV display. Figure 7a show an image with original rendering method. The condylar process of mandible and the mandibular notch shown in the circle can not be distinguished, while the image using anti-aliased method with oversampling and low-pass-filter is improved (Fig. 7b).

Intra-operatively, IV image overlay technique with corresponding image registration can help with the navigation by providing a broader view of the operation field [7]. In combination with robotic and surgical instrument, it even can supply guidance by pre-defining the path of a biopsy needle or by preventing the surgical instruments from moving into critical regions.

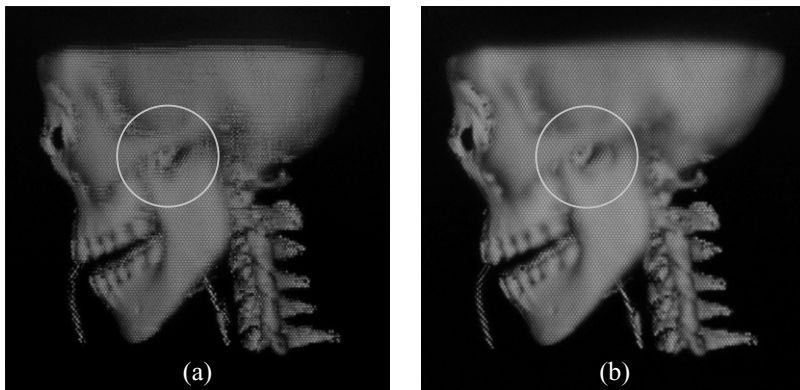


Fig. 7. Improvement of IV image quality. (a) with fundamental rendering methods; (b) with anti-aliased rendering algorithm.

4 Discussions and Conclusion

We describe a high quality image rendering for anti-aliased IV imaging by use of oversampling and low-pass-filtering techniques. The merits of developed methods are improvement of the quality of IV elemental image from single pixel to the whole elemental image. These methods directly contribute the remarkable services to the IV image formation.

The methods using for high quality IV image generation have a common weak point of computational cost. Image quality requirement of density or the resolution will increase the rendering time. Especially the IV image based on CG rendering method is time costing compared with normal CG in the same resolution of total pixels, since it is necessary to render the image for each lenslet. There are fewer connections between the rendered images of the adjacent lenses, especial when a

complex structure of object is performed. Consequently, the corresponding high speed rendering method must be brought to support the high quality IV imaging.

The display system combined with high quality IV rendering method offer a geometrical accuracy image over the projected objects (esp. depth perspective), without using the extra devices such as the wearing of special glasses. Using the proposed method, IV display enables a safe, easy, and accurate navigation.

In conclusion, we developed a high quality IV imaging algorithm and corresponding display for IV surgical display system. The feasibility study indicated that the oversampling and low-pass-filter technique for anti-aliased imaging can improve the autostereoscopic image quality. The developed display with proposed method is satisfactory and suitable in surgical diagnosis and planning setting.

Acknowledgements. The work of H. Liao was supported in part by the Japan Society for the Promotion of Science (15-11056). N. Hata was supported in part by New Energy and Industrial Technology Development Organization (NEDO) of Japan.

References

1. P. Breedveld, H. G. Stassen, D. W. Meijer, and L. P. S. Stassen, "Theoretical background and conceptual solution for depth perception and eye-hand coordination problems in laparoscopic surgery," *Minim. Invasiv. Ther.*, vol.8, pp.227-234, Aug. 1999.
2. P. Mitchell, I. D. Wilkinson, P. D. Griffiths, K. Linsley, J. Jakubowski: "A stereoscope for image-guided surgery," *British Journal of Neurosurgery*, Vol.16, No.3, pp. 261-266, 2002.
3. H. Seno, M. Mizunuma, M. Nishida, M. Inoue, A. Yanai, M. Irimoto: "3-D-CT stereoscopic imaging in maxillofacial surgery," *Journal of Computer Assisted Tomography*, Vol.23, No.2, pp.76-279, 1999.
4. B. T. Backus, M. S. Banks, R. van Ee, and J. A. Crowell: "Horizontal and vertical disparity, eye position, and stereoscopic slant perception," *Vision Research*, vol.39, pp.1143-1170, 1999.
5. M.G.Lippmann, "Epreuves reversibles donnant la sensation du relief," *J. de Phys* Vol.7, 4th series, pp821-825, 1908.
6. S.Nakajima, K.Nakamura, K.Masamune, I.Sakuma, T.Dohi, "Three-dimensional medical display with computer-generated integral photography," *Computerized Medical Imaging and Graphics*, 25, pp235-241, 2001.
7. H. Liao, N. Hata, S. Nakajima, M. Iwahara, I. Sakuma, T. Dohi, "Surgical Navigation by Autostereoscopic Image Overlay of Integral Videography," *IEEE Trans. Inform. Technol. Biomed.*, Vol.8 No.2, pp.114-121, June 2004.
8. H. Liao, N. Hata, M. Iwahara, I. Sakuma, T. Dohi, "An autostereoscopic display system for image-guided surgery using high-quality integral videography with high performance Computing," *MICCAI 2003*, LNCS 2879, pp247-255, 2003.
9. P. J. La Riviere, X.C. Pan, "Anti-aliasing weighting functions for single-slice helical CT," *IEEE Trans. Med. Imag.*, Vol.21 No.8, pp.978-990 AUG 2002.
10. J. G. Yang, S. T. Park, "An anti-aliasing algorithm for discrete wavelet transform," *MECH SYST SIGNAL PR*, Vol.17, pp.945-954, 2003.
11. K. Mueller, R. Yagel, J. J. Wheller, "Anti-aliased three-dimensional cone-beam reconstruction of low-contrast objects with algebraic methods," *IEEE Trans. Med. Imag.*, Vol.18 No.6, pp.519-537, JUN 1999.